

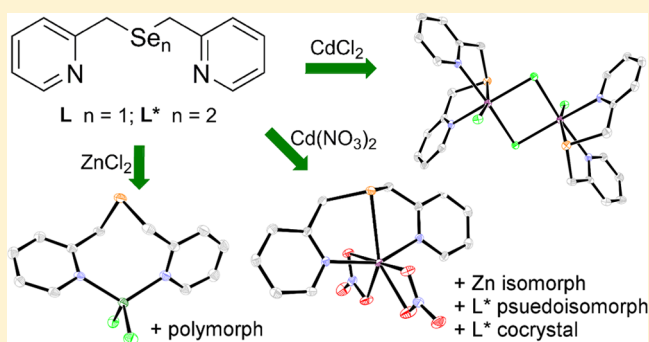
Staging Bonding between Group 12 Metal Ions and Neutral Selenium Donors: Intermolecular Interactions of Mixed N,Se Donor Ligands and Anions

Malia S. Hain, Yoko Fukuda, Carolina Rojas Ramírez, Benjamin Y. Winer, Stephanie E. Winslow, Robert D. Pike, and Deborah C. Bebout*

Department of Chemistry, The College of William & Mary, Williamsburg, Virginia 23187-8795, United States

Supporting Information

ABSTRACT: The versatile pyridyl synthons of mixed N,Se donor ligands bis(pyridin-2-ylmethyl)selane (**L**) and 1,2-bis(pyridin-2-ylmethyl)diselane (**L***) served the dual roles of metal chelating anchors and mediators of supramolecular associations in a crystallographic approach to documenting uncommon bonding between divalent Group 12 metal ions and neutral selenium functionalities. Five new molecular species with diverse ligand configurations and conformations were structurally characterized. Two macrocyclic polymorphs of $[\text{ZnLCl}_2]$ have intermolecular Se–Cl interactions rather than the desired intramolecular Zn–Se binding. Rare examples of Cd(II)-selenoether bonding are provided by tricoordinate **L** in dinuclear $[\text{CdLCl}(\mu\text{-Cl})_2]$ and mononuclear $[\text{CdL}(\mu\text{-NO}_3)_2]$. Unique intramolecular Zn-selenoether and Cd-diselenide bonds are reported for $[\text{ZnL}(\mu\text{-NO}_3)_2]$ and $[\text{CdL}^*(\mu\text{-NO}_3)_2]$, respectively. In addition, a cocrystal of $[\text{CdL}(\mu\text{-NO}_3)_2]$ and $[\text{CdL}^*(\mu\text{-NO}_3)_2]$ is structurally characterized. The intermolecular pyridyl π -interactions observed in these diverse structures are highlighted.



INTRODUCTION

Thoughtfully designed preorganized multidentate ligands have helped overcome some of the challenges associated with studies of the spectroscopically silent divalent Group 12 metal ions Zn(II) and Cd(II). These d^{10} metal ions have broad coordination number and coordination geometry tolerances, leading to rapid intermolecular exchange and intramolecular reorganization in solution. The intermolecular packing interactions of a crystal permit selective removal of a single conformation and configuration from the equilibrated molecular ensemble. In rare cases, a polymorph can be isolated permitting detailed characterization of a second species.

These and other complexities of Zn(II) and Cd(II) coordination chemistry have made it very difficult to develop accurate models of their metabolism. Zinc(II) is the second most abundant transitional metal ion in living organisms and is associated with metalloproteins belonging to each of the six fundamental classes of enzymes, playing a wide variety of structural and catalytic roles. In contrast, other than the recently discovered catalytic role for Cd(II) in the ζ class of carbonic anhydrase enzymes expressed by several marine phytoplankton in zinc-depleted environments,¹ Cd(II) is widely recognized as extremely toxic. Consideration of the full range of biomolecular coordinating groups is essential to understanding the considerable difference in biological activity of these metal ions.

Coordination chemistry studies of Group 12 metals ions have been conducted with a wide variety of N, S, and O donors, yet comparative coordination studies of Zn(II) and Cd(II) by neutral selenium donor groups have not been carried out to the best of our knowledge. Selenium is recognized as an essential trace nutrient in humans and mammals associated with cardiac health,² immunity,³ neurodegeneration prevention,⁴ and cancer suppression,⁵ among others. The selenoether L-selenomethionine (Se-met), derived from the breakdown of proteins, is the primary dietary source of selenium. Unless degraded to other selenium metabolites, Se-met is indiscriminately substituted for methionine in proteins by tRNAMet.⁶ Although substitution of the thioether methionine with the selenoether Se-met usually has no impact on overall protein structure, replacement near the active site can alter enzyme activity. For example, the Se-met-substituted phosphomannose isomerase from *Candida albicans* had a 4-fold higher K_m for substrate mannose-6-phosphate and inhibition constant for Zn(II).⁷ Diselenides are among the many metabolites responsible for selenium's biological action.⁸ In addition, a diselenide bond has been reported in a natural protein.⁹ Of relevance to this work, administration of 1,2-di(pyridin-2-yl)diselane to mice during

Received: September 17, 2014

Revised: November 4, 2014

Published: November 5, 2014

cadmium intoxication has been shown to reduce oxidative stress in various tissues.¹⁰

While deprotonated selenols (RSe^-) are bound to Zn(II) or Cd(II) in numerous structurally characterized complexes, until recently there was no published complex documenting binding of neutral selenoether (SeR_2) or diselenide (Se_2R_2) groups to either of these metal ions.¹¹ To date, the only structurally characterized example of these interactions is $[\text{CdL}_2](\text{ClO}_4)_2$ (**6**) ($\text{L} = \text{bis}(\text{pyridin-2-ylmethyl})\text{selane}$),¹² which has Cd-SeR_2 bond distances of 2.7436(4) and 2.8133(5) Å. Interestingly, the difference between the average Cd-Se and average Cd-N distances in this distorted octahedral complex could largely be accounted for by the 0.35 Å larger van der Waals radius of Se relative to N.¹³ Selenoether and diselenide functionalities present in other structurally characterized Zn(II) and Cd(II) complexes are either pendant or remote (Figures S1 and S2, Supporting Information). All the mononuclear complexes with intramolecular Zn-Se distances less than the sum of the van der Waals radii (2.01 Å for Zn^{14} and 1.90 Å for Se^{13}) share the structural feature of Zn(II) coordination to pyridyl rings with selenium at the 2-position.¹⁵ The proximity of zinc and selenium in these complexes is arguably an artifact of the rigid physical constraint associated with attachment to adjacent atoms of a pyridyl ring. The M-N-C-Se fragments of these complexes have torsion angles approaching 0° , which could allow formation of a planar four-membered ring by Zn-Se bonding (Figures S1 and S2). However, the Zn-N-C and N-C-Se bond angles are greater than 116° , relatively unstrained bond angles for sp^2 hybridized atoms. The bond angles of this fragment in a complex with Ni-Se bonding are less than 110° .¹⁶ Similarly, the Cd(II) complex of a diselenide ligand containing imidazolyl rings with selenium at the 2-position (Figure S2) has an intramolecular Cd-Se distance that is less than the sum of the van der Waals radii (2.18 Å for Cd),¹⁴ but bond angles that exceed 125° for the Cd-N-C-Se fragment, which are inconsistent with ring formation through Cd-Se bonding.¹⁷ Furthermore, other than one complex with $\pi-\pi$ stacking between head-to-tail oriented molecules producing a 3.10 Å intermolecular Zn-Se separation,¹⁸ all intermolecular Zn-Se and Cd-Se distances involving selenoethers and diselenides significantly exceed the sum of the van der Waals radii.¹¹

Our success documenting the first Cd-Se bond¹² using selenoether **L** motivated additional Group 12 coordination studies of this ligand, as well as studies of the related diselenide 1,2-bis(pyridine-2-ylmethyl)diselane (**L***) (Figure 1). These studies were facilitated by a new high yield method for synthesizing **L**.¹⁹ The common pyridyl synthon of these ligands serves as a metal anchor for entropically favorable chelation and a potential resource for intermolecular π -interactions. These chelating ligands have facial, meridional, and terminal pendant coordination modes that involve the desired M-Se bonding, as

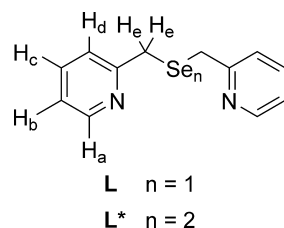


Figure 1. Potentially tridentate N_2Se ligands investigated.

well as a macrocyclic configuration without M-Se interaction (Figure 2). The sole structurally characterized, mononuclear

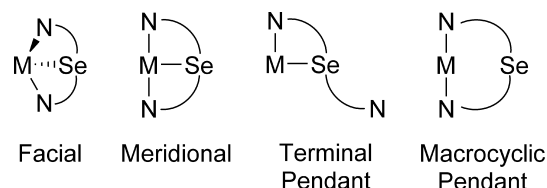


Figure 2. Configurations and conformations of N_2Se ligands in mononuclear complexes.

diselenide complex with M-Se bonds involving a chelating ligand¹¹ is the bicyclic complex $[\text{CuL}^*\text{Cl}_2] \cdot \text{CH}_2\text{Cl}_2$ with a meridional ligand configuration.²⁰ Although metal-pyridyl coordination decreases π -electron density,²¹ the pyridyl rings of this complex were suitably oriented for either intermolecular offset parallel $\pi-\pi$ interactions ($\psi = 0^\circ$, $d = 3.744$ Å; Figure 3)

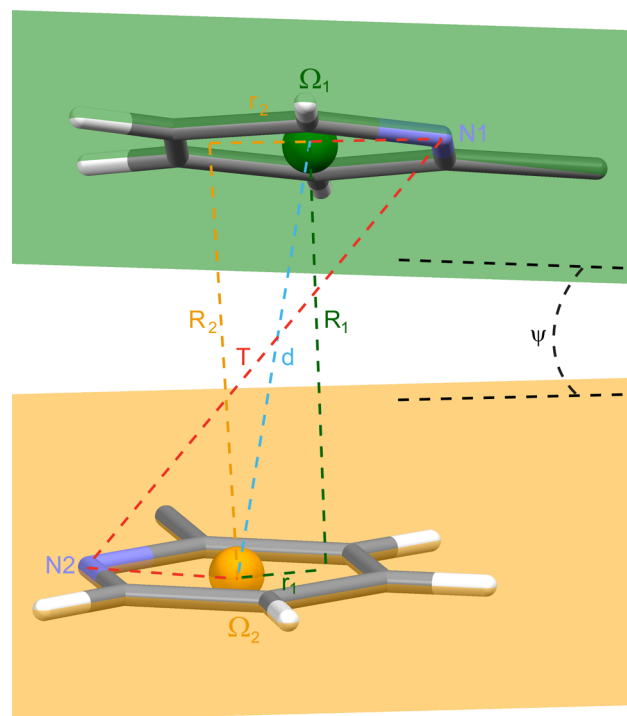


Figure 3. Geometrical parameters used for describing the stacking interactions between pyridine rings. A variation of this treatment limited to parallel pyridyl rings was reported recently by Ninković et al.²² The distance between centers of the interacting pyridyl rings is d . The angle between the planes of the pyridyl rings is ψ . The normal projection distances between the planes of the interacting rings from the centroid Ω_n is R_n . The offset (horizontal displacement) of each ring centroid from the normal projection of the other ring r_n was calculated from d and R_n . The $\Omega_1-N1-N2-\Omega_2$ torsion angles are also reported (T).

or intermolecular edge-to-face $\sigma-\pi$ interactions ($\psi = 82.1^\circ$; $d = 5.573$ Å). On the other hand, $[\text{ZnL}^*(\text{OCOC}_5\text{F}_6)_2]$ has a macrocyclic configuration with Zn-Se separation greater than 4 Å, exceeding the sum of the van der Waals radii.²³ Significantly, the later complex has close contacts between the selenium atoms and one of the electron-deficient pentafluorobenzoate anion carbons of an adjacent complex. We set out to investigate whether conditions favoring intramolecular bonding between

Table 1. Crystal Data and Refinement Results for Complexes 1–5

compound	1a	1b	2	3
emp formula	C ₁₂ H ₁₂ Cl ₂ N ₂ SeZn	C ₁₂ H ₁₂ Cl ₂ N ₂ SeZn	C ₂₄ H ₂₄ Cd ₂ Cl ₄ N ₄ Se ₂	C ₁₂ H ₁₂ N ₄ O ₆ SeZn
formula weight	399.47	399.47	892.99	452.59
temperature/K	150(2)	150(2)	100(2)	100(2)
crystal system	monoclinic	tetragonal	triclinic	triclinic
space group	C2/c	P4 ₃ 2 ₁ 2	P $\bar{1}$	P $\bar{1}$
a /Å	23.6226(10)	8.92560(10)	9.4838(2)	7.9133(2)
b /Å	8.4580(4)	8.92560(10)	10.3298(2)	8.3841(2)
c /Å	16.2905(7)	18.4297(2)	15.2472(3)	12.7127(3)
α /°	90	90	80.1220(9)	81.8816(8)
β /°	121.2470(14)	90	88.2713(10)	80.8657(7)
γ /°	90	90	78.0084(9)	65.1216(7)
V /Å ³	2782.7(2)	1468.23(3)	1439.42(4)	752.85(3)
Z	8	4	2	2
ρ_{calc} mg/mm ³	1.907	1.807	2.060	1.997
F(000)	1568	784	856	448
θ range/°	4.378–66.990	5.51–66.92	2.942–66.999	3.533–66.966
reflns collected	15011	16119	25760	12991
data/restraints/parameters	2455/0/163	1315/0/83	5004/0/325	2603/0/217
goodness-of-fit	1.168	0.916	1.020	1.037
R ₁ ^a (I > 2 σ (I))	0.0316	0.0187	0.0292	0.0262
wR ₂ ^b (I > 2 σ (I))	0.0886	0.0533	0.0731	0.0714
compound	4a	5a	4b and 5b	
emp formula	C ₁₂ H ₁₂ CdN ₄ O ₆ Se	C ₁₂ H ₁₂ CdN ₄ O ₆ Se ₂	C ₁₂ H ₁₂ CdN ₄ O ₆ Se _{1.14}	
formula weight	499.62	578.58	511.06	
temperature/K	100(2)	100(2)	100(2)	
crystal system	triclinic	triclinic	triclinic	
space group	P $\bar{1}$	P $\bar{1}$	P $\bar{1}$	
a /Å	7.9942(3)	8.06500(10)	8.0371(2)	
b /Å	8.4913(3)	8.51580(10)	8.4838(2)	
c /Å	12.7305(4)	13.8712(2)	12.9112(3)	
α /°	80.6531(15)	80.1250(6)	80.8446(9)	
β /°	79.1801(13)	81.8550(6)	80.0131(9)	
γ /°	67.1369(12)	63.4800(5)	66.1735(8)	
V /Å ³	778.28(5)	837.509(19)	789.24(3)	
Z	2	2	2	
ρ_{calc} mg/mm ³	2.132	2.294	2.151	
F(000)	484	552	494	
θ range/°	3.552–66.990	3.243–66.993	3.493–66.996	
reflns collected	13813	14982	13557	
data/restraints/parameters	2710/0/217	2910/0/226	2734/19/281	
goodness-of-fit	1.039	1.061	1.085	
R ₁ ^a (I > 2 σ (I))	0.0217	0.0268	0.0359	
wR ₂ ^b (I > 2 σ (I))	0.0557	0.0711	0.0914	

$$^a R_1 = \frac{\sum |F_o| - |F_c|}{\sum |F_o|} \text{ and } S = \frac{[\sum [w(F_o^2 - F_c^2)^2]/(n - p)]^{1/2}}{[\sum [w(F_o^2) - (F_c^2)]^2/\sum [w(F_o^2)^2]^{1/2}}.$$

neutral selenium donors and both Zn(II) and Cd(II) could be staged through judicious anion selection.

Structurally diverse complexes were prepared using the chloride and nitrate salts of Zn(II) and Cd(II). Two macrocyclic polymorphs of [ZnLCl₂] (**1a** in C2/c and **1b** in P4₃2₁2) had distorted tetrahedral N₂Cl₂ metal coordination spheres and Se–Cl close contacts rather than the desired Zn–Se bonding. [CdLCl(μ-Cl)]₂ (**2**) provided a second crystallographic example of bonding interactions between Cd(II) and a selenoether in a distorted octahedral complex. Also described are isomorphous pentagonal bipyramidal complexes [ZnL(μ-NO₃)₂] (**3**) and [CdL(μ-NO₃)₂] (**4a**), as well as a pseudoisomorph of the later complex [CdL*(μ-NO₃)₂] (**5a**), all obtained in P $\bar{1}$ with M–Se distances <3 Å. Finally, the structure of a [CdL(μ-NO₃)₂] (**4b**) and [CdL*(μ-NO₃)₂] (**5b**)

cocrystal is reported. Intermolecular pyridyl interactions were evident in the crystal packing of all the compounds except **1b**.

EXPERIMENTAL SECTION

X-ray Diffraction. Single crystals of each complex were attached to a glass fiber. Data were collected on a Bruker SMART Apex II three-circle diffractometer system with graphite monochromator, Cu K α fine-focus sealed tube ($\lambda = 1.54178$ Å) and CCD collector using φ and ω scans. The data were corrected for Lorentz and polarization effects and for absorption using SADABS.²⁴ The structures were solved by direct methods and refined on F₂ by full-matrix least-squares using the SMART Apex and SHELXL14 program package.²⁵ All non-hydrogen atoms were refined anisotropically; the hydrogen atomic positions were fixed as riding to the bonded carbons with fixed isotropic thermal parameters. Selected crystallographic data are given in Table 1. In the cocrystal, the selenide (**4b**) and diselenide (**5b**) complexes refined to

occupancies of 85.4 and 14.6%. Because of the relatively low contribution of the diselenide molecule to the electron density map, numerous restraints were necessary in its refinement. These included bond length restraints on C6B–Se2, C7B–Se3, C5B–C6B, C7B–C8B, and Cd1B–O5B. The methylene carbons were restrained to coplanarity with the pyridyl ring. Finally, each non-H atom in the diselenide (except the Se atoms) was restrained to have identical thermal parameters to its selenide counterpart.

Geometrical parameters describing the stacking interactions between pyridine rings were determined with the CCDC Mercury program, version 1.4.2.²⁶ Some newer versions of Mercury lack the ability to calculate normal projection distances between planes and centroids (R). No hydrogen bond interactions meeting the CCDC Mercury program, version 1.4.2 default definitions were found in complexes 1–5.

Powder Diffraction. Powder diffraction analysis was carried out on the instrument described above.²⁷ Samples were ground and prepared as mulls using Paratone N oil. Four 180 s frames were collected, covering 8–100° 2 θ . Frames were merged using the SMART Apex II software²⁷ and were further processed using DIFFRAC-Plus and EVA software.²⁸

Solution-State NMR Spectroscopy. Proton NMR spectra were collected in 5 mm o.d. NMR tubes on a Varian Mercury 400VX NMR or an Agilent 400-MR DD2 NMR spectrometer operating in the pulse Fourier transform mode. Calibrated autopipets were used to prepare nominally 1–5 mM solutions for variable temperature NMR measurements. The sample temperature was maintained by blowing chilled nitrogen over the NMR tube in the probe. Proton chemical shifts were measured relative to internal solvent but are reported relative to tetramethylsilane (TMS). Coupling constants are reported in Hertz. Solution NMR spectra were stable over a period of days but unstable over extended time periods.

Materials and Syntheses. Anhydrous DMF was obtained from Alfa Aesar in ChemSeal bottles. Other organic solvents and reagents were of commercial grade and either used as received or distilled from CaH₂ as indicated. Metal salts were dried under a vacuum overnight. Elemental analyses were performed by Atlantic Microlabs, Inc. of Norcross, GA.

CAUTION! 2-(Chloromethyl)pyridine hydrochloride causes skin and eye burns and is absorbed through the skin.

Bis(pyridin-2-ylmethyl)selane (L). *Method I.* A variation of the method of Kreif et al. for preparation of alkyl selenides was initially used to prepare L.²⁹ Selenium (0.39 g, 4.9 mmol) and NaBH₄ (0.37 g, 9.8 mmol) were stirred under Ar. EtOH (1.87 mL, 29.3 mmol) and dry DMF (9 mL) were added dropwise. The initially red-brown mixture became colorless with stirring over 90 min. (2-Chloromethyl)pyridine (obtained from (2-chloromethyl)pyridine hydrochloride (2.00 g, 12.2 mmol) by neutralizing with 1.22 mL of 10 M NaOH, extracting with ether (4 × 20 mL), drying with magnesium sulfate, filtering, and concentrating by distillation under argon) was added dropwise. The reaction mixture was stirred for 2–4 h. Deionized water (5 mL) was added to quench the reaction. The solution was extracted with ether (4 × 25 mL). Combined organics were dried with magnesium sulfate, filtered, and concentrated in vacuo. The residue was triturated with ether (2 × 2 mL), concentrated in vacuo, and then purified by column chromatography on alumina using 1:3 ethyl acetate:hexanes as the mobile phase. TLC plates were visualized with aqueous 1% KMnO₄, 2% Na₂SO₄. L (R_f 0.25, 0.83 g, 3.14 mmol, 64% yield) was obtained as a pale yellow oil containing trace amounts of L*.

Method II. The method of Prakash et al.¹⁹ provided L in high purity following extraction and removal of solvent in vacuo. To minimize air oxidation of the uncomplexed ligand, it was evacuated and flushed with argon before storage at 4 °C. ¹H NMR (CDCl₃): δ 8.53 (d, 2H_a, J_{HH} 4.8), 7.61 (dt, 2H_c, J_{HH} 1.9, 7.7), 7.34 (d, 2H_b, J_{HH} 7.8), 7.12 (ddd, 2H_b, J_{HH} 7.5, 5.0, 1.0), 3.92 (s, 4H_e, ²J_{HSe} 13.7); (CD₃CN) δ 8.47 (d, 2H_a, J_{HH} 5.0), 7.66 (dt, 2H_c, J_{HH} 1.8, 7.8), 7.34 (d, 2H_b, J_{HH} 7.7), 7.12 (dd, 2H_b, J_{HH} 7.6, 4.8), 3.91 (s, 4H_e, ²J_{SeH} 13.0).

1,2-Bis(pyridin-2-ylmethyl)diselane (L*). The method of Bhasin et al. was used to prepare L*.³⁰ ¹H NMR (CDCl₃): δ 8.56 (m, 2H_a),

7.62 (dt, 2H_c, J_{HH} 1.5, 7.8), 7.21–7.14 (m, 4H_{b+d}), 4.06 (s, 4H_e, ²J_{SeH} 15.3). (CD₃CN): δ 8.49 (m, 2H_a), 7.67 (dt, 2H_c, J_{HH} 1.7, 7.8), 7.24–7.18 (m, 4H_{b+d}), 4.09 (s, 4H_e, ²J_{SeH} 14.8).

Bis(pyridin-2-ylmethyl)selanedichlorozinc(II) (1a and 1b). *Method A.* ZnCl₂ (37 mg, 256 μ mol) was dissolved in a mixture of 2 mL of acetonitrile and 2 mL methanol. While stirring, a solution of L (67 mg, 255 μ mol) in 4 mL of CH₃CN was added resulting in immediate precipitation of a white solid. The solid complex was dissolved in 75 mL of CH₃CN and 1 mL of toluene was added dropwise. A trace amount of red precipitate was removed by vacuum filtration. X-ray quality crystals of monoclinic 1a were harvested after slow evaporation of ~10 mL of the solution over the course of two months. The remaining solution was evaporated down to ~5 mL under a stream of argon to recover additional 1a. Yield: 44 mg (110 μ mol, 43%). *Method B:* A solution of L (32 mg, 122 μ mol) in 4 mL of acetonitrile was slowly added to a solution of ZnCl₂ (16 mg, 117 μ mol) in 4 mL of methanol with stirring. Colorless octahedra of tetragonal 1b suitable for X-ray analysis were obtained in very low yield from the Celite filtered solution following overnight storage at –20 °C. Continued storage of the mother liquor at –20 °C provided prismatic crystals of 1a. Based on powder diffraction analysis, the isolated sample was predominantly 1a (Figure S3, Supporting Information). Yield: 21.8 mg (54.6 μ mol, 47%). MP 239 °C (dec). Anal. Calcd for C₁₂H₁₂Cl₂N₂SeZn: C 36.06, H 3.03, N 7.01. Found: C 35.68, H 2.95, N 6.95. ¹H NMR (CD₃CN, 2 mM): δ 8.90 (d, 2H_a, J_{HH} 6.6), 8.10 (dt, 2H_c, J_{HH} 1.7, 7.8), 7.68 (dd, 2H_b, J_{HH} 8.0), 7.60 (dd, 2H_b, J_{HH} 7.7, 5.5), 3.70 (s, 4H_e, ²J_{SeH} 17.5).

Bis[bis(pyridin-2-ylmethyl)selanechloro(μ -chloro)cadmium(II)] (2). A solution of L (162 mg, 0.62 mmol) in 6 mL of acetonitrile was added to a solution of CdCl₂ (58 mg, 0.32 mmol) in 6 mL of methanol with stirring, rinsing with 2 × 0.5 mL CH₃CN. The white precipitate formed upon addition was dissolved by adding 45 mL of CH₃CN in 5 mL increments with sonication. After vacuum filtration, the solution was set aside in 5 mL aliquots for slow evaporation. Colorless X-ray quality crystals (33 mg, 12% yield based on CdCl₂) appeared within 2 days. Poor quality crystals resulted when stoichiometric amounts of ligand were used. MP 155° (dec). Anal. Calcd for C₁₂H₁₂CdCl₂N₂Se: C 32.26, H 2.71, N 6.27. Found: C 32.49, H 2.66, N 6.26. ¹H NMR (CD₃CN, 2 mM): δ 8.85 (d, 2H_a, J_{HH} 5.2), 7.87 (dt, 2H_c, J_{HH} 1.6, 7.8), 7.49 (d, 2H_b, J_{HH} 8.1), 7.42 (dd, 2H_b, J_{HH} 7.7, 5.7), 4.20 (s, 4H_e, ²J_{SeH} 12.3).

Bis(pyridin-2-ylmethyl)selane(μ -nitrate)zinc(II) (3). Zn(NO₃)₂·6H₂O (56 mg, 188 μ mol) was dissolved in acetonitrile (14 mL). While stirring, a solution of L (50 mg, 190 μ mol) in 6 mL of CH₃CN was added resulting in immediate precipitation of a white solid. After stirring overnight, the precipitate was collected by centrifugation and washed by suspension in CH₃CN (43 mg, 95 μ mol, 40% yield). The supernatant was filtered through Celite and set aside for slow evaporation. X-ray quality crystals formed in 10 days. MP 170 °C (dec). Anal. Calcd for C₁₂H₁₂N₄O₆SeZn: C 31.85, H 2.67, N 12.38. Found (precipitate): C 31.86, H 2.52, N 12.25. ¹H NMR (CD₃CN, saturated, 20 °C): δ 8.66 (d, 2H_a, J_{HH} 5.5), 8.11 (dt, 2H_c, J_{HH} 1.5, 7.8), 7.71 (d, 2H_b, J_{HH} 8.1), 7.59 (dd, 2H_b, J_{HH} 7.6, 5.4), 4.01 (s, 4H_e, ²J_{SeH} 16.1).

Bis(pyridin-2-ylmethyl)selane(μ -nitrate)cadmium(II) (4a). A solution of L prepared by the method of Prakash (38 mg, 0.144 mmol) in 10 mL acetonitrile was added to a solution of Cd(NO₃)₂·4H₂O (44 mg, 0.143 mmol) in 5 mL acetonitrile with stirring, rinsing with 2 × 1 mL acetonitrile. The resulting white precipitate was either collected by centrifugation or dissolved by incremental addition of acetonitrile (4 × 5 mL) with sonication. The clarified solution was filtered through Celite and partitioned into roughly 10 mL fractions. Although no evidence for air oxidation of 4 was found by ¹H NMR after weeks of storage at room temperature in an oxygen saturated acetonitrile solution, slow evaporation was conducted under positive pressure of argon as a precaution against potential air oxidation. Small, colorless crystals appeared after 4 days and were harvested after 11 days (10 mg, 14% yield). MP 160 °C (dec). Anal. Calcd for C₁₂H₁₂CdN₄O₆Se: C 28.85, H 2.42, N 11.21. Found (precipitate): C 28.76, H 2.49, N 11.07. ¹H NMR (CD₃CN, nominally 2 mM): 8.64 (d, 2H_a, J_{HH} 5.3), 7.90 (dt,

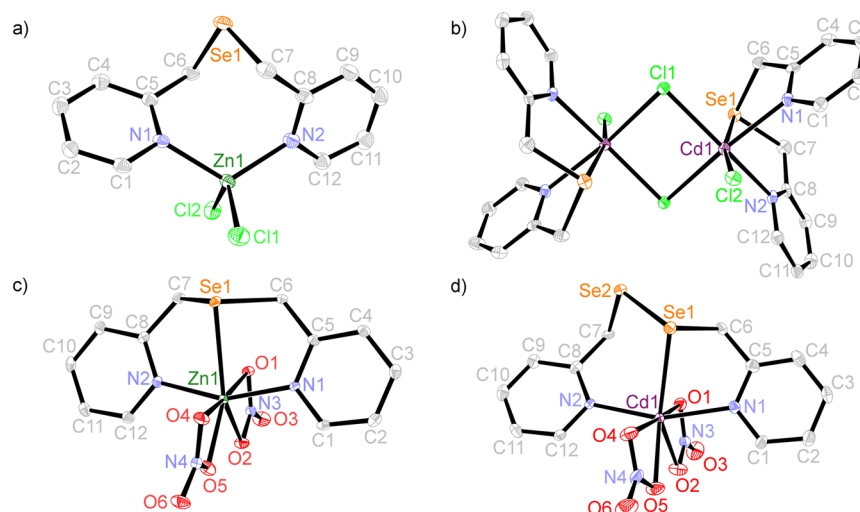


Figure 4. ORTEPs representing (a) $[\text{ZnLCl}_2]$ in $C2/c$, **1a**, (b) one of two similar $[\text{CdLCl}(\mu\text{-Cl})_2]$ complexes in **2** with labels for one side of the C_2 symmetric ion, (c) $[\text{ZnL}(\mu\text{-NO}_3)_2]$, **3**, (d) $[\text{CdL}^*(\mu\text{-NO}_3)_2]$, **5a**. Hydrogens omitted for clarity. Probability ellipsoids are shown at 50%.

$2H_c$, $J_{\text{HH}} 1.7, 7.7$), 7.53 (d, $2H_d$, $J_{\text{HH}} 7.8$), 7.45 (dd, $2H_b$, $J_{\text{HH}} 7.5, 5.5$), 4.16 (s, $4H_e$, $^2J_{\text{SeH}} 13.2$).

1,2-Bis(pyridin-2-ylmethyl)diselenedi(μ -nitrate)cadmium(II) (5a). A solution of $\text{Cd}(\text{NO}_3)_2 \cdot 4\text{H}_2\text{O}$ (31 mg, 100 μmol) in 5 mL CH_3CN was added to a solution of L^* (34 mg, 99 μmol) in 5 mL CH_3CN with stirring. During the addition, the initially clear yellow solution slowly turned reddish-pink. A light rose-brown precipitate formed while stirring the solution for 1 h. The solid residue was collected using a fine grade sintered glass vacuum funnel (30 mg, 58%). Colorless X-ray quality crystals of **5a** were obtained by slow evaporation of a Celite filtered acetonitrile (10 mL) solution of $\text{Cd}(\text{NO}_3)_2 \cdot 4\text{H}_2\text{O}$ (25 mg) and L^* (28 mg). MP: 121 $^\circ\text{C}$ (dec). Anal. Calcd for $\text{C}_{12}\text{H}_{12}\text{CdN}_4\text{O}_6\text{Se}_2$: C 24.91, H 2.09, N 9.68. Found: C 24.86, H 2.08, N 9.56. ^1H NMR (CD_3CN , nominally 2 mM): δ 8.64 (m, $2H_a$), 7.98 (dt, $2H_c$, $J_{\text{HH}} 1.7, 7.8$), 7.54 (d, $2H_d$, $J_{\text{HH}} 7.8$), 7.54–7.50 (m, $2H_b$), 4.22 (s, $4H_e$, $^2J_{\text{SeH}} 17.8$).

Cocrystal of $[\text{CdL}(\mu\text{-NO}_3)_2]$ (4b) and $[\text{CdL}^*(\mu\text{-NO}_3)_2]$ (5b). An acetonitrile (10 mL) solution of L (50 mg, 0.190 mmol; prepared by variation of the method of Kreif) was added to an acetonitrile (5 mL) solution of $\text{Cd}(\text{NO}_3)_2 \cdot 4\text{H}_2\text{O}$ (58 mg, 0.188 mmol) with stirring, rinsing with 2×1 mL acetonitrile. A turbid pink suspension formed. After stirring overnight, an off-white precipitate was removed by centrifugation (51 mg). The ^1H NMR of the initial precipitate matched **4a** with no detectable **5**. The pale yellow supernatant was set aside for slow evaporation. Several milligrams of X-ray quality crystals formed in 2 weeks. MP 109 $^\circ\text{C}$ (dec). Optimal refinement of two separate molecules required 85.4% **4** and 14.6% **5** composition, reproducible for different crystals. Insufficient crystalline material was obtained for elemental analysis. The ^1H NMR of the crystalline material was consistent with the mixed ligand composition determined by X-ray crystallography (Figure S3). ^1H NMR (CD_3CN , nominally 2 mM): 8.66 (d, $1.74 H_a$, $J_{\text{HH}} 5.3$), 8.60 (d, $0.18 H_a^*$, $J_{\text{HH}} 5.1$), 7.92 (dt with downfield shoulder, $2.00 H_{c+c^*}$, $J_{\text{HH}} 1.6, 7.7$), 7.54 (d, $1.80 H_d$, $J_{\text{HH}} 7.9$), 7.46 (dd with downfield shoulder, $2.20 H_{b+b^*+d^*}$, $J_{\text{HH}} 7.7, 5.3$), 4.17 (s, $4.18 H_{e+e^*}$, $^2J_{\text{SeH}} 13.0$).

RESULTS

The ligands chosen for this study were prepared in one step from commercially available starting materials. Five crystal structures of individual 1:1 metal:ligand complexes of ZnCl_2 , CdCl_2 , $\text{Zn}(\text{NO}_3)_2$ and $\text{Cd}(\text{NO}_3)_2$ and one cocrystal are described in this section with reference to their molecular conformations and configurations, intermolecular close contacts and π -interactions. Recent analysis of the π -interactions between parallel pyridine rings²² has been extended with

additional parameters to accommodate nonparallel pyridyl rings (Figure 3). The atom color scheme in crystal packing diagrams is the same as that in the ORTEPs. Selected ORTEPs of individual complexes are given in Figure 4a–d. The details of crystal structure solution and refinement are given in Table 1. Metal–selenium and average metal–nitrogen distances are highlighted in Table 2. Selected bond lengths and angles

Table 2. Metal–Selenium and Average Metal–Nitrogen Distances in New Compounds

metal	ligand	compound	M–Se (Å)	average M–N (Å)
Zn	L	1a	4.1829(5)	2.065(14)
		1b	4.1579(7)	2.056(2)
		3	2.7775(4)	2.061(15)
Cd	L	2a	2.8294(4)	2.39(3)
		2b	2.8715(5)	2.395(16)
		4a	2.8679(3)	2.257(4)
		4b	2.8739(16)	2.250(12)
	L*	5a	2.8979(4)	2.290(16)
		5b	2.891(12)	2.33(6)

(Tables S1–S3) as well intermolecular short contacts (Tables S5 and S6) are tabulated in the Supporting Information. Pairs of pyridyl rings with centroid-to-centroid distances (d) less than 5.5 Å were evaluated for edge-to-face σ – π (generally $60^\circ < \psi < 120^\circ$) and face-to-face or offset face-to-face π – π ($3.3 \text{ Å} < R < 3.9 \text{ Å}$ and $\psi < 30^\circ$) interactions.³¹

Crystal Structures of $[\text{ZnLCl}_2]$ Polymorphs **1a** and **1b**.

The prevalent polymorph of $[\text{ZnLCl}_2]$ crystallized in $C2/c$ (**1a**, Figure 4a). This asymmetric conformation has a Co(II) isomorph.³² One of several crystallization attempts at 4 $^\circ\text{C}$ initially produced a trace amount of the C_2 symmetric polymorph **1b** in $P4_32_12$. There is a Co(II) isomorph³³ of the later complex. The ZnCl_2 complex of bis(pyridine-2-ylmethyl)sulfane (**7**) crystallizes in $P4_22_12$ with similar cell parameters, macrocyclic configuration, and metal coordination sphere to **1b**.³⁴ An overlay of **1a** and **1b** (Figure 5a) reveals highly similar macrocyclic structures with N_2Cl_2 metal coordination spheres. The Zn(II)–Se distances exceeded 4 Å in the two complexes (Table 2). The powder diffraction pattern of bulk material isolated after extended storage at low

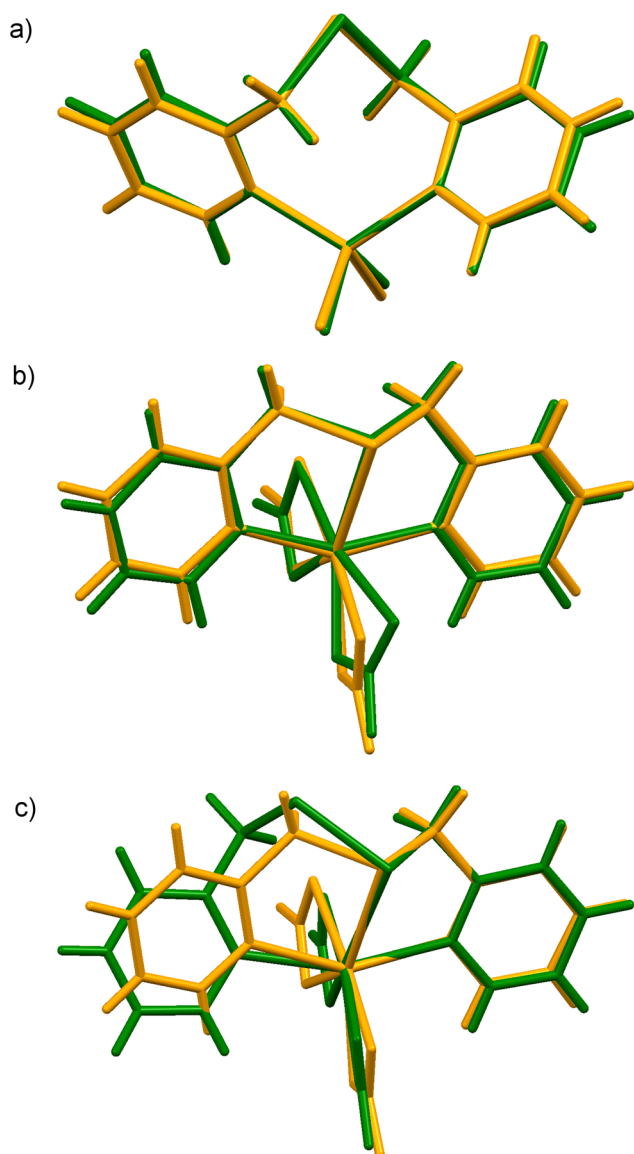


Figure 5. Selected overlays of new complexes. (a) N–Zn–N overlay (rms 0.009 Å) of [ZnLCl₂] in C2/*c* (**1a**, green) and P4₃2₁2 (**1b**, orange), (b) N–M–N overlay (rms 0.15 Å) of [ZnL(NO₃)₂] (**3**, green) and [CdL(NO₃)₂] (**4a**, orange), (c) Cd–Se–C–C–N chelate ring overlay (rms 0.09 Å) of [CdL*(NO₃)₂] (**5a**, green) and **4a** (orange).

temperature matched the pattern predicted for **1a** (Figure S5a, Supporting Information). Although the predicted powder diffraction features of **1b** had extensive overlap with the experimental data (Figure S5b), predicted peaks at 2θ values of 20.46, 32.04 and 41.70° were poorly accounted for in the experimental data. On the basis of these results, the bulk material was predominantly the higher density form **1a** (Table 1), consistent with the general thermodynamic principals governing polymorph stability of ordered molecular solids with intermolecular interactions dominated by van der Waals forces.³⁵

Although **1a** and **1b** have very similar twist-boat macrocyclic ring conformations (Figure 5a, Table S4),³⁶ there are extensive differences in intermolecular interactions (Figure 6; Table S5). The pendant selenium atom in **1a** has a single 3.4389(9) Å close contact with Cl1 (van der Waals radius 1.75 Å),¹³ forming

extended chains of molecules along the *b* axis (Figure 6a). A parallel ($\psi = 14.5^\circ$) displaced aromatic stacking interaction between N2 pyridyl rings with centroid separation 3.740 Å was observed (Table 3). The normal distance *R* for parallel displaced rings was 3.53 Å, well within the range of 3.0–4.0 Å observed for structures involving free pyridines.³² In addition, each N2 ring is involved in both intra- and interchain edge-to-face π – π interactions with N1 pyridyl rings. These remarkably similar interactions ($\psi = 56.8^\circ$; $d \approx 4.8$ Å) involve opposite faces of the N1 pyridyl rings. In contrast, the pendant selenium atom in **1b** has a pair of 3.5143(9) Å close contacts with Cl1 from adjacent molecules forming extended helices along the *c* axis (Figure 6b). The pyridyl rings of **1b** are poorly oriented for any type of π – π interaction ($\psi = 45.6^\circ$; $d = 4.865$ Å). The closely related sulfane complex **7** had neither S–Cl close contacts nor pyridyl rings with suitable orientation for π – π interactions ($\psi = 43.6^\circ$; $d = 4.875$ Å).

Crystal Structure of [CdLCl(μ -Cl)]₂ (2**).** Complex **2** crystallized in $P\bar{1}$ as a pair of similar (μ -Cl)₂ bridged dimers (Figure 4b) located at crystallographic inversion centers. The distorted octahedral Cd(II) ions have N₂Cl₃Se coordination with the selenium located trans to the terminal chloride. The Cd–Se bond distances are well within the sum of the van der Waals radii (Table 2). Facial three-coordinate L has $85^\circ < \text{N–M–N} < 96^\circ$ angles and $\psi \sim 60^\circ$ in **2**, similar to the conformation found in the homoleptic bis-chelate [CdL₂](ClO₄)₂ (**6**).¹² The average Cd–Se and Cd–N bonds in **2** and **6** are comparable. The fused five-membered chelate rings in **2** have a flattened envelope conformation with the methylene carbons in the flap positions. The Cd(II) chloride complex of bis(pyridine-2-ylmethyl)sulfane has a form isomorphic³⁴ to **2** and a form crystallizing in $P2_1/n$.³⁷

The two types of dimers in **2** are stacked upon themselves down the crystallographic *b* axis with crystallographic inversion centers between adjacent molecules. The puckered L on the ends of each dimer have pyridyl rings nestled against a ligand associated with the other dimer such that the pyridyl rings form a crude tetrahedron (average face-edge-face angle of 65(15)°). The N1 pyridyl rings are involved in edge-to-face interactions with one N3 pyridyl and face-to-edge σ – π interactions with a pair of N4 pyridyl rings (Figure 7). Close contacts between neighboring molecules include a pair of Cl–H for each terminal Cl and one Cl–H for each bridging Cl (Table S5).

Crystal Structures of [ZnL(μ -NO₃)₂] (3**) and [CdL(μ -NO₃)₂] (**4a**).** Isomorphs **3** (Figure 4c) and **4a** crystallized in $P\bar{1}$ with similar molecular structures (Figure 5b). The metal ions have pentagonal bipyramidal N₂O₄Se coordination spheres. The M–Se bond distances (Table 2) are well within the sum of the van der Waals radii. The selenide ligand adopts a meridional configuration with N1–M–N2 angles 156.36(9)° and 150.78(8)°, respectively, and $\psi < 5^\circ$. The fused five-membered chelate rings both have an envelope conformation with the Se atom in the flap position. Nearly coplanar bidentate nitrate anions and selenium occupy the equatorial plane. The M–O bonds for the oxygens closer to selenium are longer than those for the more distant oxygens. Interestingly, the Zn–N bond lengths in **1a** and **3** are nearly identical despite the considerable differences in the rest of the metal coordination sphere and ligand configuration (Table 2). In contrast, the Cd–N bond lengths are shorter and Cd–Se bond lengths longer in **4a** than in all their counterparts in **2** and **6**. Significantly, **3** is the very first structurally characterized complex with Zn–Se bonding, and these are the first complexes with meridional L.^{12,19}

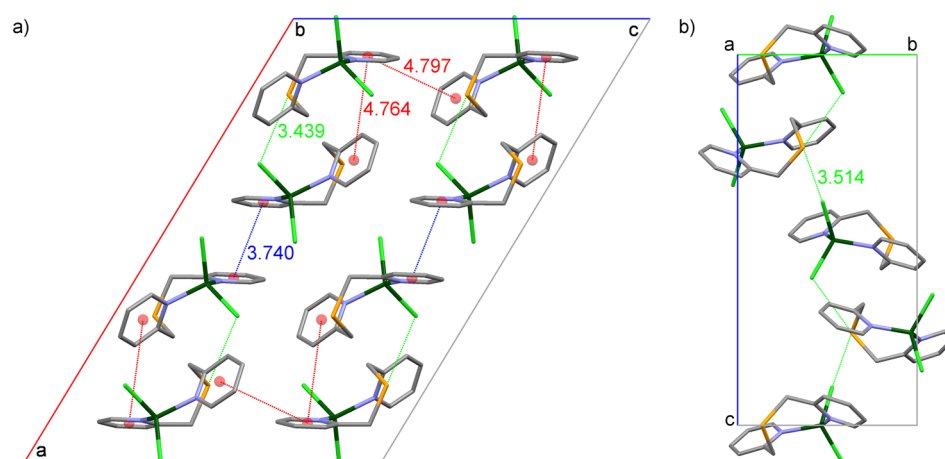


Figure 6. Packing diagrams highlighting intermolecular interactions in (a) **1a** viewed down the *b* axis and (b) **1b** viewed down the *a* axis. Hydrogens omitted for clarity. Close Se–Cl interactions are shown in lime green. Centroid–centroid distances are shown in blue for face-to-face π – π stacking interactions (parallel displaced) and in red for edge-to-face σ – π aromatic interactions.

Table 3. Geometric Parameters for π Interactions in **1–5**

compound	rings	ψ ($^\circ$)	$ \tau $ ($^\circ$)	d (Å)	R_1 (Å)	R_2 (Å)	r_1 (Å)	r_2 (Å)
1a	N2–N2'	14.5	35.5	3.74	3.53	3.53	1.25	1.25
	N1–N2'	56.8	76.6	4.76	4.74	2.15	0.53	4.25
	N1''–N2'	56.8	61.9	4.80	1.89	4.58	4.41	1.42
2	N1–N3'	61.7	129.7	4.69	4.59	1.86	0.96	4.31
	N1–N4'	59.0	110.0	4.75	3.07	4.66	3.62	0.89
	N1–N4''	59.0	104.5	4.76	2.93	4.58	3.75	1.30
3	N1–N1'	0.0	180.0	3.87	3.72	3.72	1.06	1.06
	N1'–N2''	4.3	154.4	3.72	3.49	3.45	1.39	1.26
	N2''–N2'''	0.0	180.0	3.81	3.40	3.40	1.72	1.72
4a	N1–N1'	0.0	180.0	3.65	3.33	3.33	1.50	1.50
	N1'–N2''	4.2	145.8	3.70	3.42	3.47	1.29	1.41
	N2''–N2'''	0.0	180.0	3.79	3.68	3.68	0.89	0.89
5a	N1–N1'	0.0	180.0	3.78	3.34	3.34	1.77	1.77
	N1'–N2''	20.1	161.0	4.01	3.58	3.96	1.82	0.65
	N2''–N2'''	0.0	180.0	3.69	3.43	3.43	1.36	1.34

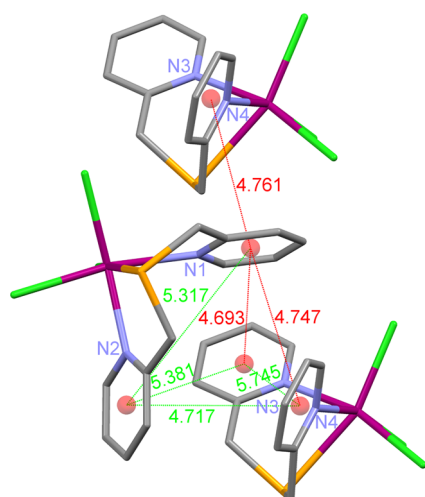


Figure 7. Packing diagram for **2** highlighting intermolecular edge-to-face σ – π aromatic interactions between similar dimers (red) and other centroid-to-centroid dimensions of dimer interface (lime green). Hydrogens and inversion related portions of the three molecules shown omitted for clarity.

Compounds **3** and **4a** have comparable layered structures. In one dimension, molecules with antioriented equatorial planes have the inequivalent pyridyl rings of **L** aligned head–head/tail–tail and approximately coplanar into strands without intermolecular contact. Two dimensional sheets (Figure 8) are formed through stairstep offset adjacent strands aligned for cross-linking parallel π – π interactions. The geometric features of the three distinct π – π interactions are provided in Table 3. There were also a number of close contacts between nitrate oxygens and pyridyl hydrogens of molecules in adjacent strands and adjacent sheets that likely contribute to the overall stability of the structure (Table S6). Several intermolecular close contacts between Se and closed shell hydrogen and/or carbon atoms from neighboring molecules may sterically advantage M–Se bonding (Table S6).

Crystal Structure of $[\text{CdL}^*(\mu\text{-NO}_3)_2]$ (5a**).** Compound **5a** crystallized in $P\bar{1}$ as a pseudoisomorph of **4a**. The pentagonal bipyramidal $\text{N}_2\text{O}_4\text{Se}$ coordination environment in this complex provides the first example of Cd–Se bonding involving a diselenide (Table 2). Interestingly, there are no structurally characterized transition metal complexes of the homologous disulfide ligand 1,2-bis(pyridin-2-ylmethyl)disulfane.¹¹ The meridionally configured **L*** has a larger N1–Cd–N2 bite angle ($159.10(10)^\circ$) and ψ (20.1°) than observed for **L** in **4a**

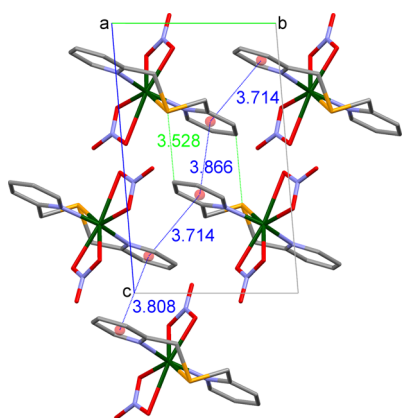


Figure 8. Packing diagram for **3** viewed down the *a* axis. Hydrogens omitted for clarity. Sheet forming offset intermolecular face to face π - π aromatic interactions are shown with their centroid distances (Å) highlighted in blue. A Se-C close contact is highlighted in green. Packing was very similar in the isomorph **4a** and pseudoisomorph **5a** (Table 3).

(Figure 5c). The five-membered chelate ring has an envelope conformation with the Se atom in the flap position, and the six-membered chelate ring has a boat conformation with cadmium and the methylene carbon in the flagpole positions. The Cd-Se and Cd-N bond lengths are slightly longer in **5a** than in **4a** (Table 2), while the average Cd-O are nearly identical (Table S3). The three-dimensional structure of **5a** consists of sheets with offset parallel π - π interactions comparable to **4a** (Table 3). The nitrate oxygens of **5a** have some close contacts with the free Se in addition to those with pyridyl hydrogens (Table S6).

The only other structurally characterized complex of **L*** with M-Se bonding is $[\text{CuL}^*\text{Cl}_2]\cdot\text{CH}_2\text{Cl}_2$ (**8**).²⁰ The overall conformation of the ligands is similar in **5a** and **8**. The Cd-Se bond length is 0.276 Å longer than the Cu-Se bond length, exceeding the difference in their van der Waals radii by 0.056 Å.¹⁴ Published structures for six other mononuclear complexes with M-Se bonding involving a diselenide were found in the Cambridge Crystallographic Database.¹¹ Among these complexes, **5a** has the longest M-Se distance (Table S7). The Se-Se bond distances in these complexes were within the range observed for free diselenides and have no clear trend with the length of the M-Se bond.

Cocrystal Structure of $[\text{CdL}(\mu\text{-NO}_3)_2]$ (4b**) and $[\text{CdL}^*(\mu\text{-NO}_3)_2]$ (**5b**).** The initial procedure used for preparing **L** based on the method of Krief et al.²⁹ produced varying amounts of **L*** as a contaminant. Improvements made to the method reduced **L*** contamination to <5% based on ¹H NMR integration. Initial attempts to prepare **4** were conducted using a modest amount of acetonitrile, resulting in considerable precipitation. Removal of the precipitate for characterization by elemental analysis and ¹H NMR provided a supernatant inadvertently enriched with **L*** complex. Slow evaporation of the supernatant provided crystalline material for which the X-ray structure showed the electron density peaks expected for **4** with the addition of two anomalous electron density peaks in the difference map. The peaks were roughly the size of oxygen atoms and in the general vicinity of Se1. Observation of these anomalous electron density peaks in a second crystal of this material, but not in pure **4**, suggested they were not caused by inadequately corrected absorption, Fourier series truncation errors or radiation damage. Furthermore, the distance between these

peaks matched the bond distance expected for a diselenide. Additional refinement with a modest number of restraints uncovered a minor component in excellent structural agreement with the diselenide complex **5** isolated independently.

Refinement using SHELX provided a cocrystal composition of approximately 85% **4** and 15% **5** (Figure 9). The mole

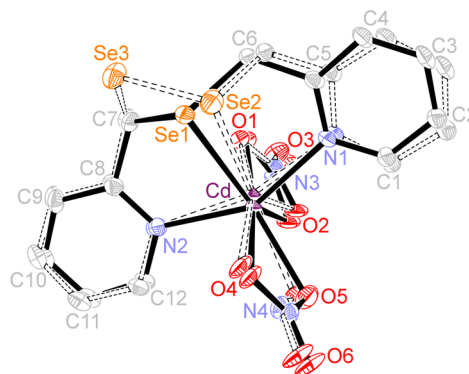


Figure 9. Ortep overlay of **4b** (solid bonds; Se1) and **5b** (dashed bonds; Se2 and Se3) as cocrystallized. Only one atom label has been provided for atoms the molecules have in common. Hydrogens omitted for clarity.

fraction weighted molecular volume of the individual components was comparable to the molecular volume of the cocrystal. On the basis of the refined composition, comparative CHN analyses of **4** and the cocrystal would be expected to have a relative difference of only 2.2%, well within acceptable tolerances. Fortunately, the chemical shifts of H_a and H_d for **4** and **5** are sufficiently different to confirm that the bulk contribution of **5** to the cocrystals was in the range of 9–15% (Figure S3). Forcing refinement with a 90:10 ratio of **4**:**5** to evaluate the composition range suggested by proton NMR resulted in essentially the same structures for the components, but a lower quality structure ($R_1 = 4.34\%$; $wR_2 = 10.58\%$; GOF = 1.210). Since the geometric parameters of the complexes were slightly different in the cocrystal than in the pure crystalline materials, the cocrystalline complexes are referred to as **4b** (Figure S6a) and **5b** (Figure S6b).

While intentional stoichiometric cocrystallization has become an active area of research for the formulation of drugs with improved physicochemical properties,³⁸ the tendency of solute mixtures to form homogeneous molecular solids is relied upon every time recrystallization is employed as a method of purification.³⁹ In the case of **4** and **5**, their pseudoisomorphous relationship thwarted separation by crystallization. The geometric parameters of **4a** and **4b** have very modest differences (Table S3), with a rms deviation in non-hydrogen atom locations of 0.026 Å (Figure S6a). The Cd1-Se1 and Cd-N2 bond distances of **4** were slightly shortened, and the Cd1-N1 bond distance was unchanged by cocrystallization with **5**. In contrast, the Cd1-N1 bond distance of **5** was slightly shortened, while the other two metal-ligand bond distances were elongated by more than 0.09 Å through cocrystallization. Inserting **5** into a crystalline matrix of **4** resulted in a ligand conformation with rms deviations of 0.11 Å for the N1-C1-C2-C3-C4-C5-C6-Se2 and 0.22 Å for the N2-C12-C11-C10-C9-C8-C7-Se2 portions of **L*** with respect to the independent complex. In contrast, the ligand rms deviations for **L** between **4** in its independent and cocrystalline forms were roughly an order of magnitude smaller but were also somewhat

larger for the N2 side of the ligand. These observations are consistent with a solid solution⁴⁰ in which the minor component **5b** is surrounded by **4b**.

Homogeneous **4a** and **5a** each have three distinct pyridyl ring π - π interfaces (Table 3). On the basis of the observed distances between centers of the interacting pyridyl rings (d) and angles between the planes of the pyridyl rings (ψ) distances, supramolecular interactions between homologous (N1–N1' and N2–N2' in both **4a** and **5a**) and pseudohomologous (N1–N2 of **4a**) pyridyl rings have similar geometric parameters, while the nonhomologous interface of the N2 and N1 pyridyl rings of **5a** has the most distinct geometric parameters. The N1 pyridyl ring of **5b** likely readily emulates both its pseudohomologous counterparts in **4b**, resulting in cocrystalline components with more modest differences between the N1 pyridyl ring side of the homogeneous and cocrystallized species. In contrast, the N2 pyridyl ring of **5b** in the cocrystal no longer interacts with a homologous component from an adjacent molecule. Instead, the N2 pyridyl ring of **5b** encounters nonhomologous π - π interactions on both sides from the N1 and N2 pyridyl rings of **4**, resulting in the more substantial structural perturbations observed.

DISCUSSION

The d¹⁰ metal ions investigated are notoriously difficult to investigate in solution because they tolerate a variety of coordination numbers and geometries resulting in rapid intramolecular isomerization and intermolecular exchange. Readily synthesized potentially tridentate ligands with demonstrated selenium–metal coordination abilities^{12,20} were chosen for this study to help suppress coordinative pliancy and limit solution speciation. Purposeful anion variations set the stage for the first crystallographic characterization of intramolecular bonding interactions between Zn(II) and a selenoether and between Cd(II) and a diselenide. Additional rare Cd–SR₂ bonds were also documented in this manner.

In addition to serving as metal anchors for chelation, the ligand pyridyl synthons served as mediators of supramolecular associations, influencing ligand conformation and configuration. Pyridines have electron poor ring systems with permanent dipoles. Coordination of a positively charged metal ion to a pyridine nitrogen enhances both the dipole strength and electron deficiency of the ring, enhancing stabilizing contributions from antiparallel dipole alignment and decreasing π - π repulsion for stacked rings.²¹ Significantly, torsions angles (T) approaching 180° were frequently observed between pyridyl rings with interpyridyl angle $\psi \approx 0^\circ$ in the new complexes reported here (Table 3). Furthermore, the normal distance R for face-to-face pyridyl rings was typically less than 4 Å, the range associated with stabilizing π - π interactions between pyridine rings.²² Meridional ligand coordination was especially favorable for parallel offset aromatic interactions and generated a large ligand bite angle (Table S3) that imposed greater restrictions on the location of the central coordinating atom, thereby favoring M–Se coordination over long-range Se interactions. In contrast, facial ligand coordination was associated with edge-to-face aromatic interactions while the macrocyclic ligand configuration led to a combination of the two types of aromatic interactions. In all the complexes, there were close contacts between electronegative elements and the electron-depleted periphery of the pyridyl rings.

The potentially tridentate organic ligands used in this work form one-to-one metal to ligand complexes requiring additional

ligands to complete the metal coordination sphere. The observed ligand configurations and conformations varied with the steric demands of the bound counterions. The modest steric demands of two chlorides allowed an N–M–N angle over 115° and twisting of the pyridyl rings of **L** in opposite directions to establish large Ω_1 –N₁–N₂– Ω_2 intramolecular torsion angles for **1a** and **1b**. This ligand conformation keeps the coordination number of the small Zn(II) ion low while constraining the central selenium to a pendant location accessible to intermolecular contacts. The tripod of chlorides associated with the bis(μ_2 -chloro)dichlorodcadmium(II) core of **3** sterically compresses the N–M–N angle toward 90°, which is not compatible with any of the common conformations of a *cis,cis*-1,4-cyclooctadiene ring (Figure S4).³⁶ The smaller N–M–N angle constrains the intramolecular torsion angle to small values and the reasonably large Cd(II) ion readily accommodated the octahedral coordination environment associated with selenium ligation trans to the terminal chloride. Interestingly, there is no crystallographic precedent for binding of a tridentate ligand to a bis(μ_2 -chloro)dichlorodizinc(II) core.¹¹ The terminal chlorides of this moiety are commonly bent away from the Zn₂Cl₂ ring reducing the surface area available for binding to other ligands. Complexes **3**–**5** had a pair of nearly coplanar μ -nitrates occupying a meridional surface roughly orthogonal to the extended ligand. The O1–M–O4 bond angles exceeded 165°, sterically restricting intramolecular pyridyl ring torsion of orthogonal **L** and **L*** bound in an extended fashion with N–M–N angles exceeded 150°. Selenium bonding along the meridional plane to form two fused chelate rings was favored over a macrocyclic conformation.

Importantly, this work establishes that bonding interactions are possible between Zn(II) and selenoethers and between Cd(II) and diselenides. Both these functionalities occur naturally in biological molecules. While physiological metal ion concentrations are normally kept quite low by high affinity metal binding groups, Se–Met is incorporated into organs with high rates of protein synthesis including the liver, kidney, stomach, and gastrointestinal mucosa.⁴¹ Since organs responsible for the metabolism, storage, and excretion of metal ions are also prevalent sites for Se–met protein incorporation, the selenoether coordination chemistry of both physiologically essential and toxic metal ions has potential biological relevance. The neutral selenium functionalities investigated in this work can be part of metal chelating environments when incorporated into proteins, potentially enhancing the opportunities for M–Se interaction. In this context, further studies to evaluate possible roles for selenoethers and diselenides in the considerable biological activity differences between Zn(II) and Cd(II) are supported.

CONCLUSIONS

In this work, the challenge of documenting direct coordination of a selenoether with Zn(II) and Cd(II) and a diselenide with Cd(II) was successfully staged using a crystallographic approach, avoiding the ambiguity that plagues solution studies of d¹⁰ metal ions. Additional rare Cd–SR₂ bonds were also documented. Crystallization of the d¹⁰ metal complexes extricated a single molecular structure from the mélange likely present in solution. Potentially tridentate ligands provided preorganization that was favorable for M–Se coordination but not sufficient. Pyridyl synthons effectively served dual roles as metal anchors for chelation and mediators of supramolecular

associations influencing ligand conformation and configuration. In addition to edge-to-face and offset face-to-face interactions between pyridyl rings, the electron-deficient periphery of the pyridyl rings was engaged in intermolecular close contacts with the anions. Besides participating in these potentially stabilizing interactions, sterically demanding anion arrangements completed the stage for ligand conformations involving M–Se binding.

■ ASSOCIATED CONTENT

■ Supporting Information

Schematics for structurally characterized complexes of Zn(II) and Cd(II) with organic molecules containing SeR₂ and RSeSeR moieties, tables of geometrical parameters (bond lengths, bond angles, torsion angles, and close contacts) for studied compounds, powder diffraction of **1a**, ¹H NMR of cocrystallized **4b** with **5b** and overlays of **4b** with **4a** and **5b** with **5a**. X-ray crystallographic information files (CIF) are available for compounds **1a**, **1b**, **2**, **3**, **4a**, **5a**, and the cocrystal (**4b** and **5b**). This material is available free of charge via the Internet at <http://pubs.acs.org>. Crystallographic information files are also available from the Cambridge Crystallographic Data Center (CCDC) upon request (<http://www.ccdc.cam.ac.uk>, CCDC deposition numbers 1024857, 1024858, 1032554, and 104860–1024863).

■ AUTHOR INFORMATION

■ Corresponding Author

*Phone: (757) 221-2558. Fax 757-221-2715. E-mail: dcebo@wm.edu

■ Author Contributions

The manuscript was written through contributions of all authors. All authors have given approval to the final version of the manuscript.

■ Notes

The authors declare no competing financial interest.

■ ACKNOWLEDGMENTS

This work was supported in part by the U.S. National Science Foundation Division of Chemistry under Grants 0315934 and 0750119. Purchases of the College of William & Mary SMART Apex II diffractometer and Agilent 400-MR DD2 NMR spectrometer were supported by the National Science Foundation (Grants 0443345 and 1337295, respectively), as well as The College of William & Mary. Additional support for undergraduate co-workers was provided by a Howard Hughes Medical Institute grant through an Undergraduate Biological Sciences Education Program Award to the College of William and Mary.

■ REFERENCES

- (1) Xu, Y.; Feng, L.; Jeffrey, P. D.; Shi, Y.; Morel, F. M. *Nature* **2008**, *452*, 56–61.
- (2) Tanguy, S.; Grauzam, S.; de Leiris, J.; Boucher, F. *Mol. Nutr. Food Res.* **2012**, *56*, 1106–1121.
- (3) Mocchegiani, E.; Costarelli, L.; Giacconi, R.; Malavolta, M.; Basso, A.; Piacenza, F.; Ostan, R.; Cevenini, E.; Gonos, E. S.; Monti, D. *Mech. Ageing Dev.* **2014**, *136*–137, 29–49.
- (4) Pitts, M. W.; Byrns, C. N.; Ogawa-Wong, A. N.; Kremer, P.; Berry, M. J. *Biol. Trace Elem. Res.* **2014**, *161*, 231–245.
- (5) Wallenberg, M.; Misra, S.; Bjoernstedt, M. *Basic Clin. Pharmacol. Toxicol.* **2014**, *114*, 377–386.
- (6) Schrauzer, G. N. *J. Nutr.* **2000**, *130*, 1653–1656.

(7) Bernard, A. R.; Wells, T. N.; Cleasby, A.; Borlat, F.; Payton, M. A.; Proudfoot, A. E. *Eur. J. Biochem.* **1995**, *230*, 111–118.

(8) Weekley, C. M.; Harris, H. H. *Chem. Soc. Rev.* **2013**, *42*, 8870–8894.

(9) Shchedrina, V. A.; Novoselov, S. V.; Malinoski, M. Y.; Gladyshev, V. N. *Proc. Natl. Acad. Sci. U. S. A.* **2007**, *104* (13919–13924), S13919/1–S13919/11.

(10) Luchese, C.; Zeni, G.; Rocha, J. B. T.; Nogueira, C. W.; Santos, F. W. *Chem.-Biol. Interact.* **2007**, *165*, 127–37.

(11) Cambridge Structural Database (v 5.35 updated November 2013).

(12) Winer, B. Y.; Berry, S. M.; Pike, R. D.; Bebout, D. C. *Polyhedron* **2012**, *48*, 125–130.

(13) Bondi, A. J. *Phys. Chem.* **1964**, *68*, 441–51.

(14) Hu, S.-Z.; Zhou, Z.-H.; Robertson, B. E. *Z. Kristallogr.* **2009**, *224*, 375–383.

(15) (a) Thöne, C.; Narro, P.; Jones, G. 2010, Private communication to the Cambridge Structural Database, deposition number CCDC 767272. (b) Kienitz, C. O.; Thöne, C.; Jones, P. G. *Z. Naturforsch., B: Chem. Sci.* **2000**, *55*, 587–596. (c) Kienitz, C. O.; Thöne, C.; Jones, P. G. *Inorg. Chem.* **1996**, *35*, 3990–3997. (d) Thöne, C.; Narro, P.; Jones, G. 2010, Private communication to the Cambridge Structural Database, deposition number CCDC 768229.

(16) Thöne, C.; Narro, P.; Jones, G. 2010, Private communication to the Cambridge Structural Database, deposition number CCDC 767273.

(17) Kedarnath, G.; Kumbhare, L. B.; Jain, V. K.; Wadawale, A.; Dey, G. K.; Thinaharan, C.; Naveen, S.; Sridhar, M. A.; Prasad, J. S. *Bull. Chem. Soc. Jpn.* **2008**, *81*, 489–494.

(18) Dochnahl, M.; Löhnwitz, K.; Lühl, A.; Pissarek, J.-W.; Biyikal, M.; Roesky, P. W.; Blechert, S. *Organometallics* **2010**, *29*, 2637–2645.

(19) Prakash, O.; Sharma, K. N.; Joshi, H.; Gupta, P. L.; Singh, A. K. *Dalton Trans.* **2013**, *42*, 8736–8747.

(20) Thöne, C.; Narro, P.; Jones, G. 2010, Private communication to the Cambridge Structural Database, deposition number CCDC 767270.

(21) Janiak, C. *J. Chem. Soc., Dalton Trans.* **2000**, 885–8896.

(22) Ninković, D. B.; Janjić, G. V.; Zarić, S. D. *Cryst. Growth Des.* **2012**, *12*, 1060–1063.

(23) Thöne, C.; Vancea, F.; Jones, P. G. 2010, Private communication to the Cambridge Structural Database, deposition number CCDC 766453.

(24) (a) SAINT Plus, Data Reduction Software, version 7.34a; Bruker AXS Inc: Madison, WI, 2005;. (b) Sheldrick, G. M. SADABS; University of Göttingen: Göttingen, Germany, 2005.

(25) (a) Sheldrick, G. M. *Acta Crystallogr., Sect. A: Found. Crystallogr.* **2008**, *64*, 112–22. (b) Sheldrick, G. M. SHELXS 97,, version 6.14; Universität Göttingen: Germany, 1997.

(26) Bruno, I. J.; Cole, J. C.; Edgington, P. R.; Kessler, M.; Macrae, C. F.; McCabe, P.; Pearson, J.; Taylor, R. *Acta Crystallogr., B* **2002**, *58*, 389–397.

(27) SMART Apex II, Data Collection Software, version 2.1; Bruker AXS Inc: Madison, WI, 2005.

(28) DIFFRAC Plus, version 10.0 and EVA, release 2004, Bruker AXS Inc.: Madison, WI, 2005, 2005.

(29) Krief, A.; Trabelsi, M.; Dumont, W.; Derock, M. *Synlett* **2004**, 1751–1754.

(30) Bhasin, K. K.; Singh, J.; Singh, K. N. *Phosphorus Sulfur Silicon Relat. Elem.* **2002**, *177*, 597–603.

(31) Loots, L.; Barbour, L. J. A Rudimentary Method for Classification of π - π Packing Motifs for Aromatic Molecules. In *The Importance of Pi-Interactions in Crystal Engineering*; Tiekink, E. R. T.; Zukerman-Schpector, J., Eds.; John Wiley & Sons, Ltd.: West Sussex, UK, 2012; pp 109–124.

(32) Thöne, C.; Narro, P.; Jones, G. 2010, Private communication to the Cambridge Structural Database, deposition number CCDC 767493.

- (33) Thöne, C.; Narro, P.; Jones, G. 2010, Private communication to the Cambridge Structural Database, deposition number CCDC 767276.
- (34) Berry, S. M.; Bebout, D. C.; Butcher, R. J. *Inorg. Chem.* **2005**, *44*, 27–39.
- (35) (a) Kitaigorodskii, A. I. *Organic Chemical Crystallography*; Consultants Bureau: New York, 1961. (b) Bernstein, J. *Polymorphism in Molecular Crystals*; Oxford University Press: 2002.
- (36) Anet, F. A. L.; Yavari, I. *J. Am. Chem. Soc.* **1977**, *99*, 6986–6991.
- (37) Sung, N.-D.; Choi, K.-Y.; Lee, H.-H.; Lee, K.-C.; Kim, M.-J. *Transition Metal Chem.* **2005**, *30*, 273–277.
- (38) Schultheiss, N.; Newman, A. *Cryst. Growth Des.* **2009**, *9*, 2950–2967.
- (39) Aakeröy, C. B.; Salmon, D. J. *CrystEngComm* **2005**, *7*, 439–448.
- (40) Inoue, K.; Tohnai, N.; Miyata, M.; Matsumoto, A.; Tani, T.; Goto, Y.; Shinkai, S.; Sada, K. *Cryst. Growth Des.* **2009**, *9*, 1072–1076.
- (41) Hansson, E.; Jacobsson, S.-O. *Biochim. Biophys. Acta* **1966**, *115*, 285–293.